Characterization and Modeling of Small-Signal Substrate Resistance Effect in RF CMOS

Yo-Sheng Lin, Shey-Shi Lu*, *Senior Member, IEEE*, Tai-Hsing Lee and Hsiao-Bin Liang

Department of Electrical Engineering, National Chi-Nan University, Puli, Taiwan, R.O.C.
Tel: 886-4-92910960 ext.4101, Fax: 886-4-92917810, Email : stephenlin@ncnu.edu.tw
*Department of Electrical Engineering, National Taiwan University, Taipei, R.O.C.

Abstract — **A novel theory based on dual-feedback circuit methodology is proposed to explain the kink phenomenon of scattering parameter S_{22} in deep submicrometer MOSFETs. Our results show that the output impedance of MOSFETs intrinsically shows a series RC circuit (for low substrate resistance) or a "shifted" series RC circuit (for very high substrate resistance) at low frequencies, and a parallel RC circuit at high frequencies. It is this inherent triple characteristic of the output impedance that causes the appearance of double kinks phenomenon of S_{22} in a Smith chart. Our model can not only predict the behavior of S_{22}, but also calculate all S-parameters accurately. Experimental data of 0.25-μm-gate MOSFETs are used to verify our theory. Excellent agreement between theoretical values and experimental data was found.**

I. INTRODUCTION

Transistor scattering parameters (S-parameters) have been used extensively in active microwave circuit design. However, some behaviors of transistor S-parameters are still not fully understood, for example, the kink phenomenon of the scattering parameter S_{22} of deep submicrometer MOSFETs with high substrate resistance [1]. This is because it was thought that S_{22} should roughly follow a constant conductance circle in the Smith chart. Furthermore, it is strange that this kink phenomenon is invisible when the substrate resistance of a MOSFET is small, but only becomes apparent when the substrate resistance of a MOSFET is large. Traditionally, transistor S-parameters are mostly understood in terms of Y- or Z-parameters. These Y- or Z-parameters, though very useful in calculating S-parameters, cannot provide insight into the behavior or physical meaning of the S-parameters. In this paper, we present a novel theory to explain these mysterious characteristics by deriving the output impedance (or admittance) of a MOSFET under the measurement conditions of S-parameters.

II Theory

The setup for the measurement of transistor S-parameter is shown in Fig. 1, where Z_O (= $1/Y_O$) = 50 Ω is connected to the input and output ports of the device-under-test. If the expression for the output impedance Z_{out} of this circuit has been found, then S_{22} is given by

$$S_{22} = \frac{Z_{out} - Z_O}{Z_{out} + Z_O}. \quad (1)$$

The circuit configuration, in general, is too complicated to find its output impedance. Nevertheless, if this circuit is viewed as a dual feedback circuit in which R_s is the local series-series feedback element and C_{gd} is the local shunt-shunt feedback element, then the problem becomes much more tractable. For simplicity, all the inductors in Fig. 1 are temporarily neglected. We will refer to them in later discussions in Section III. From local series-series feedback theory [2], [3], the circuit of Fig. 1 can be transformed into that of Fig. 2 with some necessary circuit element modifications as follows: $C'_{gs} = C_{gs}/(1 + g_m R_s)$, $R'_i = R_i + R_s$, $C'_{ds} = C_{ds}/(1 + g_m R_s)$, $R'_{ds} = R_{ds}(1 + g_m R_s)$, $C'_{gd} = C_{gd}$, $g'_m = g_m/(1 + g_m R_s)$, $g'_{mb} = g_{mb}/(1 + g_m R_s)$, $C'_{bd} = C_{bd}/(1 + g_m R_s)$, $C'_{bs} = C_{bs}/(1 + g_m R_s)$, $R'_b = R_b(1 + g_m R_s)$.

Note the circuit in Fig. 2 is much easier to handle. We can define an "intrinsic output impedance" $Z_{out,i}$ as

$$Z_{out,\,i} = Z_{out,\,i1} \| Z_{out,\,i2} \quad (2)$$

where the symbol $\|$ represents parallel combination. The expression of impedances $Z_{out,\,i1}$ and $Z_{out,\,i2}$ can easily be obtained from local shunt-shunt theory [3] and is given by

$$Z_{out,\,i1} = \frac{(sC''_{gs} + \frac{1}{Z_{O1}})^{-1} + \frac{1}{sC'_{gd}}}{1 + g''_m (sC''_{gs} + \frac{1}{Z_{O1}})^{-1}} = \frac{1 + s(C''_{gs} + C'_{gd})Z_{O1}}{(1 + g''_m Z_{O1})sC'_{gd} + s^2 C''_{gs} C'_{gd} Z_{O1}} \quad (3)$$

0-7803-7246-8/02/$10.00 © 2002 IEEE

$$Z_{out,\,i2} = \frac{(sC'_{bs} + \frac{1}{R'_b})^{-1} + \frac{1}{sC'_{bd}}}{1 + g'_{mb}(sC'_{bs} + \frac{1}{R'_b})^{-1}}$$

$$= \frac{1 + s(C'_{bs} + C'_{bd})R'_b}{(1 + g'_{mb}R'_b)sC'_{bd} + s^2 C'_{bs}C'_{bd}R'_b} \quad (4)$$

where $C''_{gs} = C'_{gs}/(1 + sR'_i C'_{gs})$, $g''_m = g'_m/(1 + sR'_i C'_{gs})$, and $Z_{O1} = Z_O + R_g$. The normal output impedance is the parallel combination of $Z_{out,\,i}$, C'_{ds} and R'_{ds} followed by a series combination with R_d as follows:

$$Z_{out} = (Z_{out,\,i} \left\| \frac{1}{sC'_{ds}} \right\| R'_{ds}) + R_d . \quad (5)$$

From (5), S_{22} can be determined according to (1). We now turn our attention to S_{11}. According to local shunt-shunt feedback theory [3], it can be easily proven that the input impedance $Z_{in,\,M}$ seen to the right-hand side of C'_{gs} and R'_i (or C_{gs} and R_i) is given by

$$Z_{in,\,M} = \frac{\frac{1}{sC'_{gd}} + Z_L}{1 + g''_m Z_L} = \frac{1}{s(1 + g''_m Z_L)C'_{gd}} + \frac{Z_L}{1 + g''_m Z_L} \quad (6)$$

where Z_L is the parallel combination of $Z_O + R_d$, R'_{ds}, C'_{ds}, and $Z_{out,\,i2}$. From (6), S_{11} can be determined by

$$S_{11} = \frac{Z_{in} - Z_O}{Z_{in} + Z_O} = \frac{R_g + Z_{in,\,i} - Z_O}{R_g + Z_{in,\,i} + Z_O} \quad (7)$$

where $Z_{in} = R_g + Z_{in,\,i}$ and $Z_{in,\,i} = [Z_{in,\,M} \| (R'_i + 1/sC'_{gs})]$ is the input impedance seen to the right-hand side of R_g. As for S_{21}, the physical meaning of it is twice the voltage gain V_{O2}/V_1. Hence, it can easily be expressed in terms of $Z_{in,\,i}$, g''_m, C'_{gd}, R_d, R_g, Z_L, and Z_O as follows:

$$S_{21} = -2 \cdot \frac{Z_{in,\,i}}{Z_O + R_g + Z_{in,\,i}} \cdot (g''_m - sC'_{gd}) \cdot \frac{Z_L \cdot \frac{1}{sC'_{gd}}}{Z_L + \frac{1}{sC'_{gd}}} \cdot \frac{Z_O}{Z_O + R_d} . \quad (8)$$

The physical meaning of S_{12}, on the other hand, is twice the reverse voltage gain V_{O1}/V_2. It is given as follows by inspecting Fig. 2:

$$S_{12} = 2 \frac{Z_{out,\,i} \left\| R'_{ds} \right\| \frac{1}{sC'_{ds}}}{Z_{out,\,i} \left\| R'_{ds} \right\| \frac{1}{sC'_{ds}} + R_d + Z_O} \cdot \frac{sC'_{gd}}{sC'_{gd} + sC''_{gs} + \frac{1}{Z_O + R_g}} \cdot \frac{Z_O}{Z_O + R_g} . \quad (9)$$

III. EXPERIMENTAL RESULTS AND DISCUSSIONS

To verify our theory, we have applied (1)-(9) to 0.25-μm-gate MOSFETs in the calculations of their S-parameters. The effect of the inductors in Fig. 1, which we neglected previously in Section II, can be easily included by replacing R_g, R_s, R_d and R_b with $R_g + j\omega L_g$, $R_s + j\omega L_s$, $R_d + j\omega L_d$ and $R_b + j\omega L_b$ respectively. Excellent agreement between the calculated values and experimental results is found, as shown in Fig. 3 and 4. If we extend the calculated data to 40 GHz, as the dash lines shown in Fig. 3, we can clearly see the kink phenomenon appears at about 20 GHz. The reason that the kink phenomenon appears at frequency high to about 20 GHz is because both the substrate resistance (270.2 Ω) and the gate width (80 μm) of the MOSFET are too small. The kink effect will gradually become visible when the device size is increased, as was demonstrated experimentally and theoretically in Ref. [2]. In addition, the kink effect will also become more and more visible at lower frequency when the substrate resistance is increased, as was demonstrated experimentally by our experimental results in Fig. 4. The reason for the enhancement will become clear after the following discussion.

In order to explore the origin of the kink phenomenon observed in Fig. 3 and 4 for MOSFETs, (2) for the intrinsic output impedance has to be reexamined more closely. To get more insight into (2), let us assume that R'_i is negligibly small, which is usually the case. After some simple mathematical manipulation, we find that, at high frequencies, $Z_{out,\,i}$ approaches a parallel RC network, while at low frequencies and $R'_b << 1/|j\omega C'_{bs}|$ (which is usually the case), it can be approximated by a series RC network. In addition, at low frequencies and $R'_b >> 1/|j\omega C'_{bs}|$, it can be approximated by a series RC network parallel to a resistance r'_2. That is, at high frequencies

$$Y_{out,\,i} = \frac{1}{Z_{out,\,i}} = \frac{1}{Z_{out,\,1i}} + \frac{1}{Z_{out,\,2i}}$$

$$\approx \left[Y_{O1} \left(\frac{C'_{gd}}{C'_{gs} + C'_{gd}} \right)^2 + g'_m \frac{C'_{gd}}{C'_{gs} + C'_{gd}} \right]$$

$$+ \left[Y'_b \left(\frac{C'_{bd}}{C'_{bs} + C'_{bd}} \right)^2 + g'_{mb} \frac{C'_{bd}}{C'_{bs} + C'_{bd}} \right]$$

$$+ j\omega \left(\frac{C'_{gs} C'_{gd}}{C'_{gs} + C'_{gd}} + \frac{C'_{bs} C'_{bd}}{C'_{bs} + C'_{bd}} \right) \approx g + sC_P \quad (10)$$

while at low frequencies and $R'_b << 1/|j\omega C'_{bs}|$

$$Z_{out,\,i} = Z_{out,\,1i} \| Z_{out,\,2i}$$

$$\approx \left(\frac{Z_{O1}}{1 + g'_m Z_{O1}} + \frac{g'_m}{(Y_{O1} + g'_m)^2} \times \frac{C'_{gs}}{C'_{gd}} \right)$$

$$\cdot \left(\frac{(1 + g'_m Z_{O1}) C'_{gd}}{(1 + g'_m Z_{O1}) C'_{gd} + (1 + g'_{mb} R'_b) C'_{bd}} \right)^2$$

$$+ \left(\frac{R'_b}{1 + g'_{mb} R'_b} + \frac{g'_{mb}}{(Y'_b + g'_{mb})^2} \times \frac{C'_{bs}}{C'_{bd}} \right)$$

$$\left(\frac{(1 + g'_{mb} R'_b) C'_{bd}}{(1 + g'_m Z_{O1}) C'_{gd} + (1 + g'_{mb} R'_b) C'_{bd}} \right)^2$$

$$+ \frac{1}{j\omega [(1 + g'_m Z_{O1}) C'_{gd} + (1 + g'_{mb} R'_b) C'_{bd}]}$$

$$\approx r + \frac{1}{j\omega C_s} \quad (11)$$

In addition, at low frequencies and $R'_b >> 1/|j\omega C'_{bs}|$,

$$Z_{out,\,i} = Z_{out,\,i1} \| Z_{out,\,i2}$$

$$\approx \left\{ \left(\frac{Z_{O1}}{1 + g'_m Z_{O1}} + \frac{g'_m}{(Y_{O1} + g'_m)^2} \cdot \frac{C'_{gs}}{C'_{gd}} \right) \right.$$

$$\cdot \left(\frac{(1 + g'_m Z_{O1}) C'_{gd}}{(1 + g'_m Z_{O1}) C'_{gd} + C'_{bd} C'_{bs} / (C'_{bd} + C'_{bs})} \right)^2$$

$$\left. + \frac{1}{j\omega [(1 + g'_m Z_{O1}) C'_{gd} + C'_{bd} C'_{bs} / (C'_{bd} + C'_{bs})]} \right\}$$

$$\left\| \left(\frac{(C'_{bs} + C'_{bd}) R'_b}{g'_{mb} C'_{bd}} \right) \equiv (r'_1 + \frac{1}{j\omega C'_{s1}}) \right\| (r'_2) \quad (12)$$

The trends predicted by (10)-(12) have been verified in Fig. 5-7, where the data points have been calculated from (2) and (10)-(12). As can be seen from Fig. 5, for low substrate resistance, the intrinsic output impedance indeed follows a constant resistance (r) circle at low frequencies and then a constant conductance (g) circle at high frequencies. For median substrate resistance, the intrinsic output impedance first follows a constant r circle then a "shifted" constant r circle at low frequencies, and then a constant g circle at high frequencies, as shown in Fig. 6(b). It is this inherent triple characteristic of the intrinsic output impedance (or admittance) that causes the appearance of the kink phenomenon of S_{22} in a Smith chart. As for very high substrate resistance, the intrinsic output impedance follows a "shifted" constant r circle at low frequencies and then a constant g circle at high frequencies, as shown in Fig. 7. The trends predicted by Fig. 5 and 6 are very consistent with the experimental results shown in Fig. 3 and 4.

ACKNOWLEDGEMENT

Support from National Science Council of R.O.C. under Contract No. NSC90-2218-E260-007 is acknowledged.

REFERENCES

[1] Hans Hjelmgren and Andrej Litwin, *IEEE Trans. on Electron Devices,* vol. 48, no. 6, pp. 397-399, Feb. 2001.

[2] Shey-Shi Lu, Chinchun Meng, To-Wei Chen and Hsiao-Chin Chen, *IEEE Trans. on Microwave Theory and Techniques,* vol. 49, no. 2, pp. 333-340, Feb. 2001.

[3] P .R. Gray and R. G. Meyer, *Analysis and Design of Analog Integrated Circuits.* New York: Wiley, 1993, pp. 579-584.

[4] Yi-Jen Chan, Chia-Hung Huang, Chung-Chian Weng, and Boon-Khim Liew, *IEEE Trans. on Microwave Theory and Techniques,* vol. 46, no. 5, pp. 615-615, May 1998.

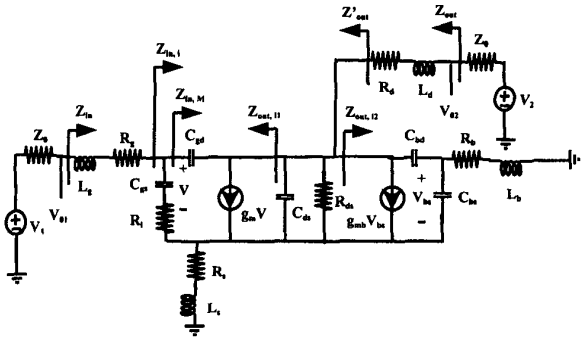

Fig. 1 Setup for the measurement of MOSFET's S-parameters: a complete circuit

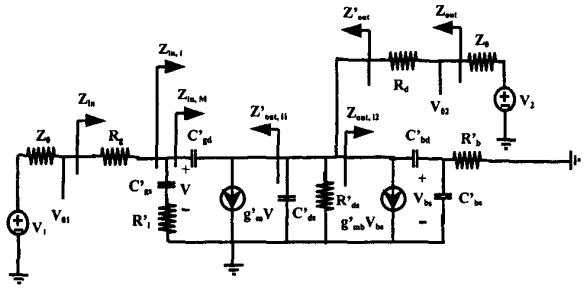

Fig. 2 Setup for the measurement of MOSFET's S-parameters: a simplified circuit with the local series-series feedback element (R_s) absorbed.

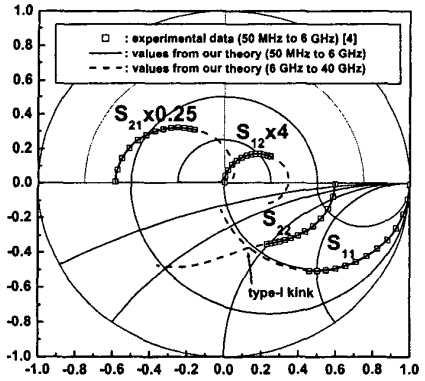

Fig. 3 Comparison between the experimental and calculated S-parameters of a 0.25-μm-gate Si MOSFET with gate length 80 μm and substrate resistance 270.2 Ω.

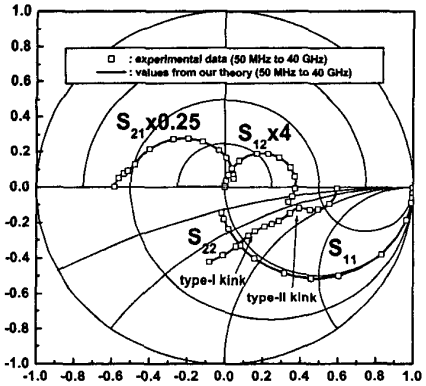

Fig. 4 Comparison between the experimental and calculated S-parameters of a 0.25-μm-gate Si MOSFET with gate length 80 μm and substrate resistance about 2000 Ω.

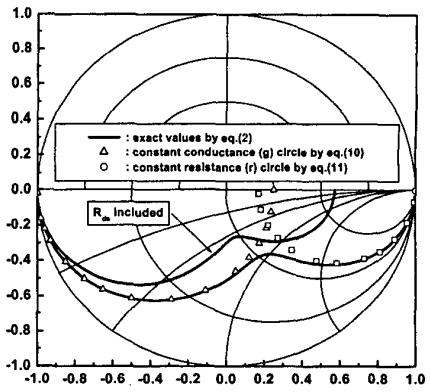

Fig. 5 When R_b is small, the intrinsic output impedance approaches a parallel RC circuit and a series RC circuit at high frequencies and low frequencies respectively.

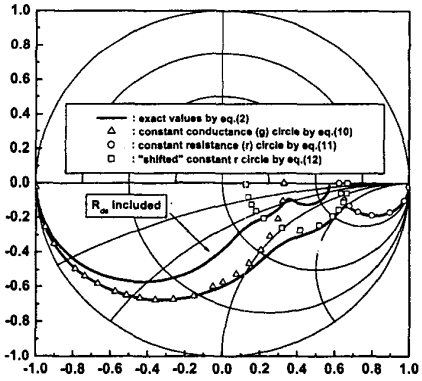

Fig. 6 When R_b is median, the intrinsic output impedance approaches a parallel RC circuit, a "shifted" series RC circuit (and a series RC circuit) at high and low frequencies respectively.

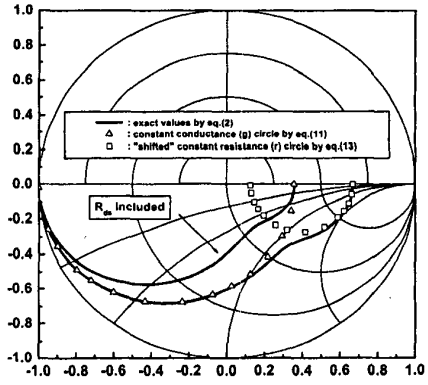

Fig. 7 When R_b is large, the intrinsic output impedance approaches a parallel RC circuit and a "shifted" series RC circuit at high and low frequencies respectively.